



Experimental investigation of blunt cone model at hypersonic Mach number 7.25

Saiprakash Mani¹ · C. Senthilkumar² · G. Kadam Sunil³ · Singh Prakash Rampratap³ · V. Shanmugam³ · G. Balu³

Received: 13 April 2020 / Accepted: 7 March 2021

© The Brazilian Society of Mechanical Sciences and Engineering 2021, corrected publication 2021

Abstract

Experiments were carried out in hypersonic shock tunnel in Defence Research and Directorate Laboratory at hypersonic Mach number of 7.25 using an 11.37° apex-angle blunt cone model. Heat flux measurement was carried out on cone model at different angles of attack with angle of rotation $\phi = 0^\circ$ to 360° in steps of 45° with vacuum sputtered platinum thin film sensors. The measured experimental value of heat transfer data at stagnation point was compared with theoretical value estimated Fay and Riddell correlation. As angle of rotation was increased from $\phi = 0^\circ$ to $\phi = 180^\circ$, the shock wave became closer to model surface due to high density ratio across the shock wave and consequently heat transfer rate became higher.

Keywords Cone model · Hypersonic flow · Platinum thin film sensors · Heat transfer · Shock waves in hypersonic flow

1 Introduction

Two outstanding features characterize the flow around the body at hypersonic speed. One is the effect of boundary layer displacement along the model, and the other is the effect of nose bluntness of the model. At hypersonic speed, boundary layers are thicker than those at lower free stream Mach

number. This is mainly because of the large temperature gradient through boundary layer that surrounds it. This large temperature gradient is produced by the kinetic energy losses that reappear in the form of internal energy of fluid. The aerodynamic heating rate will increase the surface temperature of the model. In general, stagnation point heat transfer rate is inversely proportional to the square root of nose radius and aerodynamic heating rate varies with the cube of the velocity. The shape of the body is significantly deformed by the effect of boundary layer displacement. The flow field is complicated if the leading edge is blunted. The leading edge shock causes high heating on the model surface, and this high heating rate decays with stream-wise direction.

Charless [1] tested biconic models in Langley continuous flow hypersonic tunnel to measure heat transfer rate along the model. Palladium thin film resistance heat transfer gauges were used for heat measurements. Experiments were carried out at Mach 10 with various angles of attack ranging from 0° to 20° . With the effect of Reynolds number ranging from 2.2×10^5 to 9.4×10^5 , the variation of windward heating rate along the model surface was not substantial, but large variation of heating rate was observed in the leeward side for the same variation of Reynolds number. Saito et al. [2] measured unsteady convective heat transfer rate on cylinder in a shock tube. Test was carried out at different incident shock Mach numbers ranging from 1.77 to 4.04 with different angles of rotation ϕ of 90° , 112.5° , 135° , and 180° . The flow separation occurred at angles less than 90°

Technical Editor: André Cavalieri.

✉ Saiprakash Mani
iamsaiaero@gmail.com
C. Senthilkumar
cskumarr@gmail.com
G. Kadam Sunil
kadamdrdl@gmail.com
Singh Prakash Rampratap
singhprakashdrdl@gmail.com
V. Shanmugam
shanmugamdrdl@gmail.com
G. Balu
gbaludrdl@gmail.com

¹ Department of Aerospace Engineering, MLR Institute of Technology, Hyderabad, India

² Department of Aerospace Engineering, MIT Campus, Anna University, Chennai 600044, India

³ Directorate of Aerodynamics, Defence Research and Development Laboratory, Hyderabad 500058, India

and greater than 90° for laminar flows and turbulent flows, respectively [3].

Ratan and Jagadeesh [4] carried out experiment in combustion driven shock tunnel on two parallel flat plates with a 33° wedge attached to the upstream end of the bottom plate. Gaseous hydrogen was injected at an angle 45° from a port on the bottom plate. Heat transfer rate was measured at the end of the plate and midway between the parallel plates, and the measured values were compared for the three gases, namely nitrogen, air, and oxygen rich air. Liu et al. [5] measured the heat flux distribution on blunted wave rider, including the effect of angle of attack and sideslip angle. Shimshi and Walberg [6] performed in Langley's 15-in. and 20-in. Mach 6 tunnels to investigate the aerodynamic heating to spherically blunted cones at different angles of attack. The results showed that stagnation heating rate decreased with increasing the cone half angle. Over the years, several heat transfer measurements have been reported in open literature [7–10].

Kumar [11] designed, fabricated, and tested three different types of thermal sensors (platinum material based, platinum/nanomaterial, and coaxial thermocouple). The results showed that extremely small thickness of coaxial thermocouple and platinum thin film gauges had the ability to measure heat flux where the run time of the test section was only a few milliseconds. In addition, platinum thin film sensor was capable of measuring low value of heat flux (0.1 W/cm^2) as compared to coaxial thermocouple. Hubner et al. [12] used luminescent coating techniques for the measurement of heat flux in sharp and blunt nose models. Charge-coupled device (CCD) camera was used for capturing the thermal images. Thin film resistance thermometer, coaxial surface thermocouple [13], null-point calorimeter [13], infrared thermography [14], and temperature-sensitive paints techniques [15, 16] were used to measure the heat flux. For the measurement of heat transfer rate along the model surface, fast response temperature sensors having response time of few micro sec were required. Thin film gauge is a proven technique used for the measurement of heat transfer rate in short duration facility. The thin film gauge has faster response time than the other conventional temperature sensors, and it is more suitable for the present study. Thin film gauges are not commercially available as they are made according to model configuration. In this research paper, advanced techniques like vacuum sputtering and vacuum deposition of thin film platinum sensors are used for measuring the heat transfer rate. Details of platinum thin sensors, tunnel results and the comparison of measured value with theoretical results are described. A detailed review of advanced measurement techniques includes gauge calibration, data reduction techniques and uncertainty analysis. Stagnation point correlation is also discussed for the comparison of measured values. The aim of this paper is to examine the vacuum sputtered thin film

sensors for measuring the convective heat transfer rates. Studying the heat transfer rate in the stagnation point and control surface which is the characteristic of the flow situation encountered in a blunt body is also one of the objectives in this research article. The measured heat transfer rate for the blunt body at lower stagnation enthalpy of 2 MJ/kg is inadequate in open literature. Therefore, we have initiated the study in DRDL shock tunnel to determine the surface convective heating rates for missile geometry. Experiments were carried out with helium as driver gas and air as test gas at flow Mach number of 7.25 at two different angles of attack, namely 0° and 5° with angles of rotation of 0° to 360° in steps of 45° . The main goal of the present paper is to determine the heating rate as it occurs in real circumstances. The contribution of this research paper is to provide advancements in terms of accuracy of measured value, high speed of data acquisition, and reliability of sensors. Heat transfer rate measurement and its calculations are described in detail in this paper.

2 Test model

Test model size depends on the type of conical or contoured nozzle, test section size, inviscid core of the hypersonic jet coming out of the nozzle and the nozzle exit diameter. A blunt cone model was used as vehicle configuration. The nose radius of blunt cone model was 20 mm, base diameter was 200 mm, and the length of blunt cone model was 350 mm. The test model had provision to mount eight heat flux gauges on the surface. The upper limit on the model size was limited by blockage in the test section. The blockage factor is the ratio of the plan form area of the test model to the Nozzle exit area. The blockage factor was less than 10% for both angles of attack, namely 0° and 5° . When the model is exposed to hypersonic flow, the expected force will act on the test model. Based on the expected force, the model material has been chosen. It is important to note that larger mass leads to higher noise-to-signal ratio. Hence, lighter material is chosen for model fabrication for lower noise-to-signal ratios. Lightweight aluminum alloy was used for the present investigation. Figure 1 shows the test model used for the experiment.

3 Experiments

A brief description of the experimental facility and instrumentation, shock tunnel experiments, and experiments on heat transfer rate is discussed in detail.

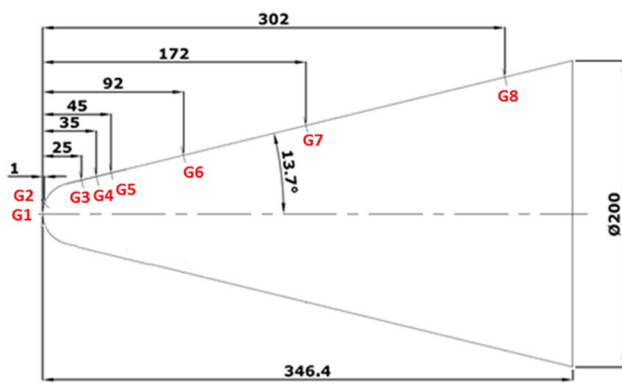


Fig. 1 Test model used for present investigation. (All dimensions are in mm)

3.1 Experimental facility and instrumentation

The experimental facility in DRDL shock tunnel had the capability to supply shock heated air at maximum stagnation pressure and maximum stagnation temperature of 100 bar and 4000 K, respectively. Helium was used as driver gas and air as driven gas and the tunnel was operated through reflected mode with convergent–divergent nozzle. The schematic view of shock tunnel is shown in Fig. 2 with the arrangement of shock tube (driver and driven section), convergent–divergent nozzle, test section, and dump tank. The shock tube had an internal diameter of 0.180 m and of length 18.5 m, and it was divided into driver and driven sections by a thin aluminum diaphragm. The aluminum diaphragm was designed to burst at a predetermined value of initial driver and driven pressure. Due to diaphragm burst, the primary shock wave travels in the shock tube with shock Mach number of M_s . When the incident shock wave reaches the vicinity of paper diaphragm, the diaphragm bursts. The incident shock wave reflects from nozzle throat and propagates towards the driver section. The incident shock Mach number is indirectly measured by using pressure transducer of 1000 psi (Model 113A24, PCB-Piezotronics, Ltd) mounted 0.52 m apart from the end of driven section. The wind tunnel portion of the shock tunnel consisted of conical nozzle terminating into the test section of 1.5 m diameter and 5 m in length, which is attached to the dump tank of about 1.8 m³.

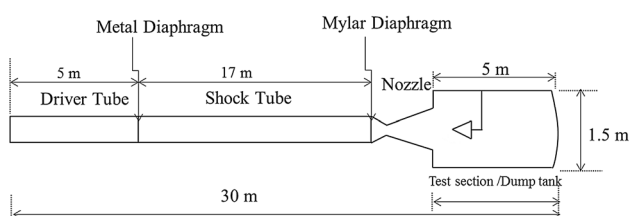


Fig. 2 The schematic view of shock tunnel

A nozzle of 10 deg cone angle with exit diameter of 1000 mm yields the flow of Mach number of 7.25. This is verified by pitot rake (six pitot probes) across the flow cross section at nozzle exit. In reflected mode of operation, free stream Mach number can be varied by using a different throat section which produces a range of Mach numbers from 6.5 to 8 and only a flow Mach of 7.25 nozzle was used for present investigation. At the same time, convergent–divergent nozzle, test section, and dump tank were evacuated to a pressure of 10⁻⁶ mill bar to reduced nozzle starting time. The shock tunnel was capable of producing the reservoir enthalpy of 4MJ/kg with the effective test time of 1.5ms [17]. The variations of reservoir pressure (P_{05}) and total pressure (P_{02}) with respect to time are shown in Figs. 3 and 4, respectively.

All the data from the data acquisition system were sampled digitally using a 14-bit multichannel system, and the data were recorded at 2.5 Mega Samples/sec/channel. Acquisition of data during the experiment was accomplished by using National instruments (NI) PXI-8187 Lab View RT controller with 2.5GHz processor speed for interrupt based trigger with a digital clock frequency of 10 MHz sampling rate.

3.2 Shock tunnel experiments

The experiment was carried out at 0° and 5° with angles of rotation of 0° to 360° in steps of 45°. The shock tunnel was operated at a stagnation enthalpy of 1.5 MJ/kg to 1.95 MJ/kg. About 20 to 25 gauges were prepared using vacuum sputtering process, and the gauges were calibrated for heat flux measurement. Some of the gauges achieved the linearity and some did not achieve the linearity due to the thickness of thin film platinum sensors and gauge resistance. The devices which achieved the linearity were

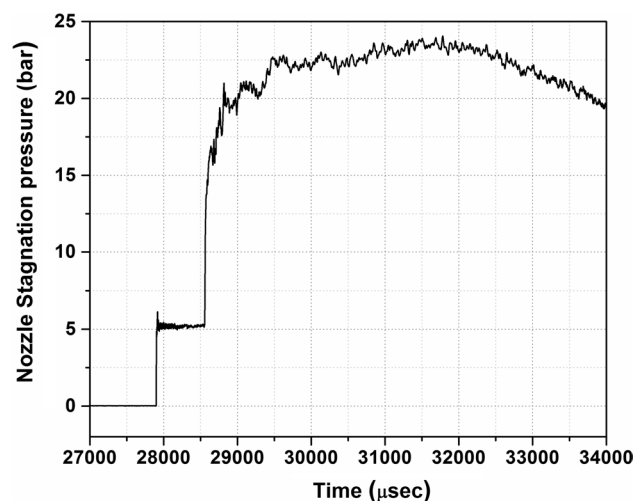


Fig. 3 Variation of stagnation pressure with respect to time

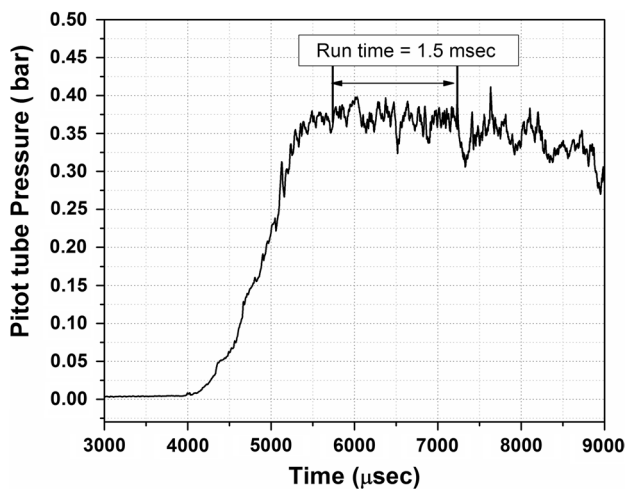


Fig. 4 Variation of Pitot pressure with respect to time

used for the present experiment. After a couple of tests, the gauges were examined for the durability of heat flux gauges. One half of the test model was with the heat flux gauges. For all the cases, the tunnel was operated with driver pressure of 43.2 to 47.48 bar and driven pressure of 0.297 to 0.32 bar (Table 1).

3.3 Heat transfer measurements

The thin film gauge consisted of thin layer of platinum film mounted on the substrate (Macor) to measure the surface heat flux on the blunt cone model. The platinum thin film gauges were developed by vacuum sputtering techniques. Then, curing of gauge at 800 °C for one hour using muffle furnace was done for getting proper adhesion and for improving bonding strength between the thin film and Macor. Electrical wire of outer diameter 0.6 mm was inserted through the hole from the bottom surface of substrate to the top surface. Silver paste was applied

between the gauge ends and electrical lead wire. Since the lead junction point was in the liquid form, it needed to undergo curing of silver paste at 150 °C for 15 min. Then resistance of cured thin film gauge was measured. The measured resistance values for all heat flux gauges were 50 to 100 Ω. The sensors were typically designed so that thickness of platinum thin film (0.4 μm) was less than the thickness of the substrate (8 mm). Hence, thin metallic film has a negligible effect on the heat conduction and the temperature measured by platinum thin film sensors (i.e. sensing element) was identical to surface temperature of the substrate. For the gauge to satisfy 1-D heat transfer theory, it is important to ensure the minimum thickness of Macor [18] for a test model to measure the surface heat transfer rate. When the gauges were exposed to high temperature flow, the change in the resistance of the gauge was proportional to surface temperature. The rate of change of heat flux was used to deduct the heat flux. The gauges were energized at constant power supply of 20 mA which was connected to data acquisition system. With the calibration curve, the gauge output with temperature gives the sensitivity of heat flux gauge. The sensitivity varies from 1.03 to 2.45 mV/°C. Cook and Felderman [19] technique was used to determine the convective heat transfer rate from voltage time history of heat flux gauge as shown in Figure 5. The numerical evaluation of the heat flux was determined from parabolic fit data along with Cook–Felderman technique. The consistent numerically evaluated heat transfer signals are shown in Fig. 6. The measured heat flux should remain constant with respect to time period of 2.8 ms due to oscillation in free stream properties in the test section of about ±5 % to 15%. The time average procedure was used to deduct the heat flux over the flight vehicle.

The measured experiment result of normalized heat transfer rate in DRDL shock tunnel for the blunt cone model is presented in Fig. 7. All the data were measured

Table 1 Test condition used for present experiment

Run number	Angle of attack	Angle of rotation	Nozzle stagnation condition	Test section condition			
	α (deg)	Φ (deg)		P_{∞} (Pa) (± 7.2)	T_{∞} (K) (± 2.0)	ρ_{∞} (kg/m ³) (± 5.9)	M_{∞} (± 1.3)
1	0	0	21.38	377.7	154	0.0088	7.21
2	0	180	21.49	376.2	162	0.0083	7.30
3	5	180	25.3	414.6	176	0.0084	7.38
4	5	0	23.93	411.8	168	0.0087	7.3
5	5	270	23.19	331.9	149	0.0077	7.49
6	5	90	22.7	376.8	160	0.0081	7.29
7	5	45	23.83	446.4	160	0.0096	7.19
8	5	225	23.33	373.0	161	0.008	7.29
9	5	315	23.62	329.1	152	0.0076	7.59
10	5	135	22.75	378.2	159	0.0082	7.42

at zero angle of attack for flow Mach number of 7.25 with Reynolds number based on the length of model which was approximately 5×10^4 . The Reynolds number in these experiments was as high as helium and used as driver gas. In Fig. 7, maximum heat transfer rate is at stagnation point and it is obtained from a model (Fig. 1) mounted at zero degree angle of attack. Thin film platinum gauges are on one half of the model. This requires the model to be rotated by 180° to get the data for the other half of the test model at the same incidence with the same condition. The experimentally measured value of heat transfer rate at the stagnation point is 53.12 W/cm^2 . Theoretically estimated stagnation point heat transfer using Fay and Riddell [20] correction is 40 W/cm^2 . The measured stagnation heat transfer value is higher than Fay–Riddell expression, and the percentage change in heat transfer rate is about 25%. This discrepancy is mainly due to the theoretical value of correlation used in Fay–Riddell expression and unsteady flow oscillation in free stream properties in the shock tunnel test section.

A blunt cone model flying at hypersonic Mach number experiences aerodynamic heating as a consequence of temperature rise through the boundary layer resulting in an increase in the temperature of vehicle skin. This gradient of temperature is produced by the kinetic energy of flight vehicle which is converted into heat energy transferring the heat from fluid medium to body surface surrounding the flight vehicle by convection. The increase in viscous boundary layer growth along the stream-wise direction from the leading edge of the blunt cone model leads to a decrease in the heat transfer rate along the stream-wise direction. Saiprakash et al. [21] investigated heat flux measurement over the sharp cone model at flow Mach of 6.56. Viscous interaction between thick boundary layer growth around the blunt cone model affects the surface

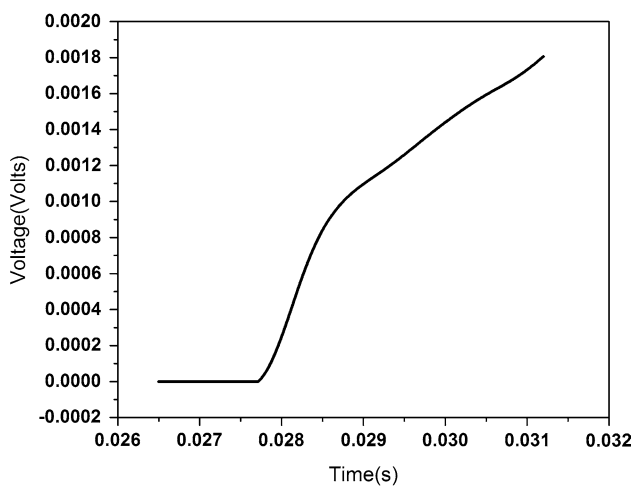


Fig. 5 Typical voltage time history of heat flux gauge (G3) for $\alpha=0^\circ$

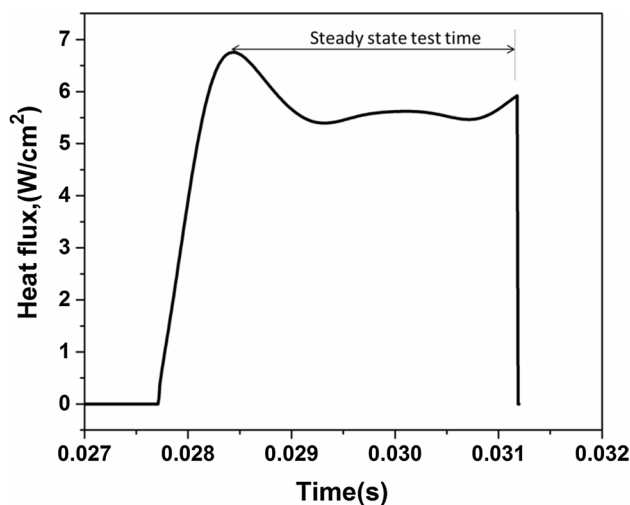


Fig. 6 Typical heat transfer signal for heat flux gauge (G3) obtained from voltage–time history

pressure distribution and stability of hypersonic flight vehicle. The percentage change in heat transfer rate from G1 to G8 is $\pm 9.5\%$ for identical test condition (i.e. windward and leeward) at zero degree angle of attack. These results clearly reflect on the quality of flow in the test section.

When the model was at 5 deg angle of attack, the maximum heat transfer rate was not observed in the windward portion of model as compared to the heat transfer rate at nose (i.e. GS1). The maximum heat transfer rate could be in the region from GS2 to GS3 where heat flux gauges were not mounted to measure the heat flux. The maximum

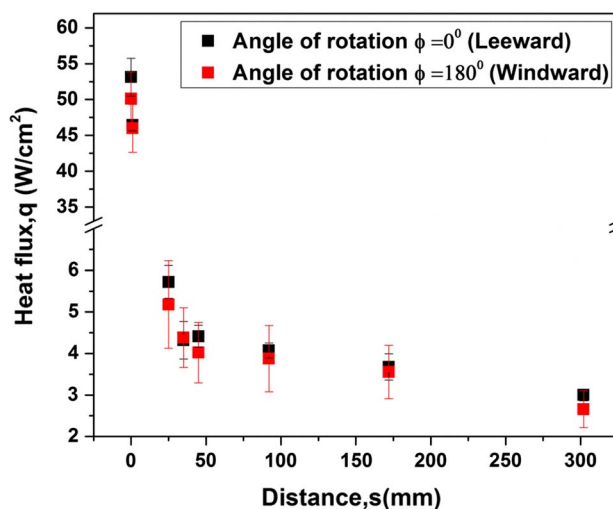


Fig. 7 Variation of convective heat flux along the length of blunt cone model at $\alpha=0^\circ$ flying at Mach 7.25 for the angles of rotation $\phi=0^\circ$ and 180°

stagnation heat transfer rate at nose was 65.8 W/cm^2 when the model was at $\alpha = 5^\circ$ for the angle of rotation $\phi = 0^\circ$ (leeward surface) and $\phi = 180^\circ$ (windward surface). It was observed that near the nose region using platinum thin film sensors the standard deviation was 2.9%, whereas for fore body, the maximum deviation was 1.2%. Away from nose, the measured heating rate decreased substantially along the stream-wise direction. At an axial location of 302 mm from the nose, the surface heating rate decreased to the minimum value (2.1% to 8.5%) of stagnation heating rate at nose. Apart from the nose region, a slight increase in aerodynamic heating was observed from an axial distance of 45 mm to 172 mm. This could be shock-boundary layer interaction at the model surface. Hence, there would be a boundary layer growth which produces both higher pressure and temperature and might lead to further growth of boundary layer. This increase in heat transfer is clearly shown in Fig. 8. The marginal separation of vortices could exist near the minimum heating rate, and reattachment can happen at high local heating rate. The increase in heat transfer was a small indication that there would be flow expansion towards the model boundary.

Due to higher density gradient and proximity of shock wave to the blunt cone model surface, the windward heating rate was higher than the leeward heating rate.

The measured local heat transfer rate at different axial locations (S) from geometric stagnation point on a blunt body is depicted in Fig. 9. The heat transfer rate is slightly higher for the angle of rotation $\phi = 90^\circ$ than for $\phi = 270^\circ$. The decrease in heating rate for $\phi = 270^\circ$ could be attributed to the slightly larger expansion of flow field than when the model was mounted at angle of rotation of $\phi = 90^\circ$. The higher heat transfer rate existed when the angle of rotation of $\phi = 180^\circ$ as compared to other angle of rotation ($\phi = 0^\circ, 45^\circ, 90^\circ, 135^\circ, 225^\circ, 270^\circ, 315^\circ$).

Figure 10 shows the average heat flux plotted along the length of the model for the two cases under study, where S represents the axial location of gauge from the nose. The heating rate in windward ray $\phi = 180^\circ$ was higher than $\phi = 135^\circ$ and $\phi = 225^\circ$. The percentage decrease in heating rate from $\phi = 180^\circ$ to $\phi = 225^\circ$ was 7.5% to 17%. Similarly from $\phi = 180^\circ$ to $\phi = 135^\circ$ was 10% to 27%. The maximum standard deviation is within $\pm 3.1\%$. The difference in heating rate for the same test condition could be due to the accumulation of moisture in the driver and the driven sections, irregularities of groove depth in metal diaphragm (i.e. aluminum) and minor diaphragm fragments which could affect the flow quality in the test section. Due to this phenomenon, the same quality and quantity of flow could not be produced even though shock tunnel was operated at the same test condition.

Figure 11 shows the variation of convective heat transfer rate along stream-wise direction of the blunt cone model at $\alpha = 5^\circ$ flying at Mach 7.25 for the angles of rotation $\phi = 45^\circ$

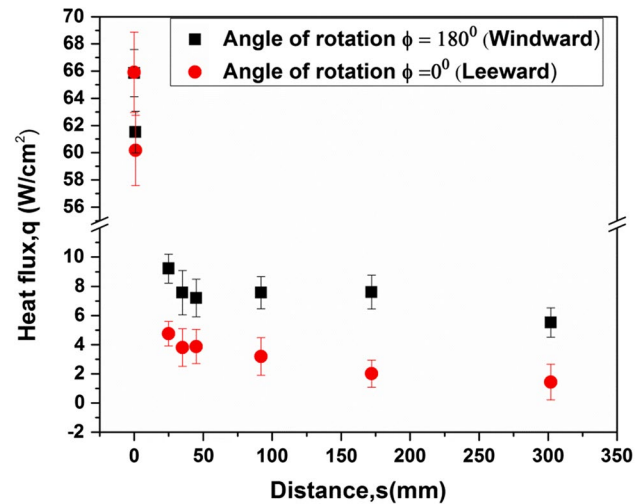


Fig. 8 Variation of convective heat flux along the length of blunt cone model at $\alpha = 5^\circ$ flying at Mach 7.25 for the angles of rotation $\phi = 0^\circ$ and 180°

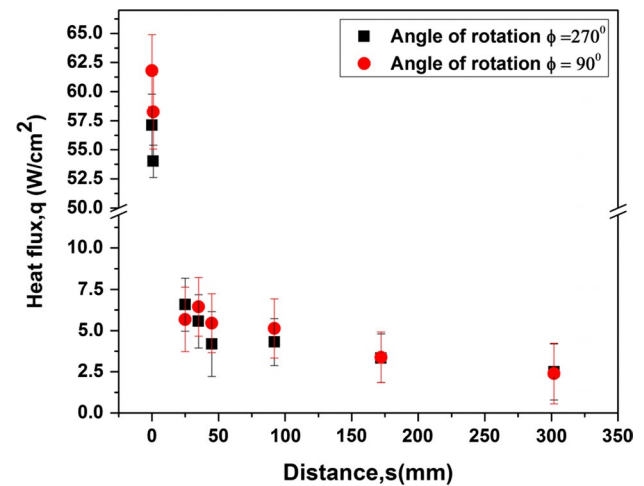


Fig. 9 Variation of convective heat flux along the length of blunt cone model at $\alpha = 5^\circ$ flying at Mach 7.25 for the angles of rotation $\phi = 90^\circ$ and 270°

and 315° . For the angle of rotation $\phi = 315^\circ$, it shows higher value of heat transfer rate than for the other case where the angle of rotation $\phi = 45^\circ$ as the flow was more compressed because of higher shock strength. The curved streamlines were no longer planer in three dimensional spaces between detached shock wave and body surface. When the angle of attack was less than flow deflection angle where $\alpha = 5^\circ < \theta_c$, the curved streamlines at $\phi = 315^\circ$ crossed stronger shock wave and attained a larger entropy than the weaker shock wave acquired for the angle of rotation $\phi = 45^\circ$ and attained lesser entropy, subsequently heat transfer rate was higher for $\phi = 315^\circ$ than for $\phi = 45^\circ$. The convective heating

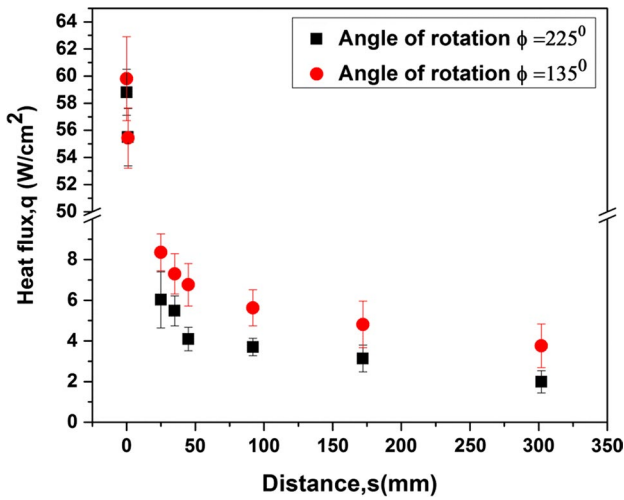


Fig. 10 Variation of convective heat flux along the length of blunt cone model at $\alpha=5^\circ$ flying at Mach 7.25 for the angles of rotation $\phi = 135^\circ$ and 225°

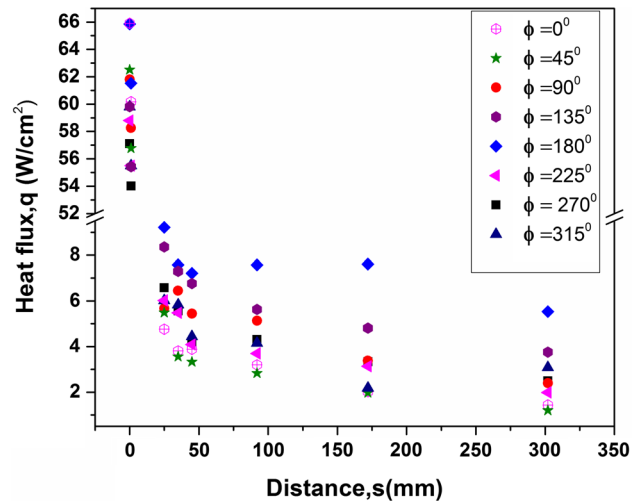


Fig. 12 Variation of convective heat flux along the length of blunt cone model at $\alpha=5^\circ$ flying at Mach 7.25 for different angles of rotation in steps of 45°

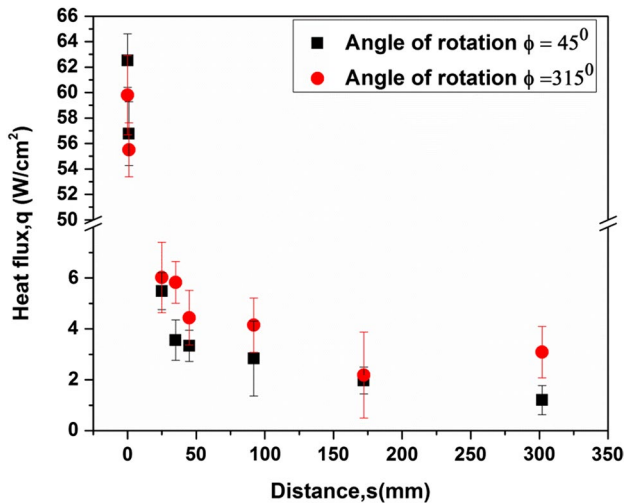


Fig. 11 Variation of convective heat flux along the length of blunt cone model at $\alpha=5^\circ$ flying at Mach 7.25 for angles of rotation $\phi = 45^\circ$ and 315°

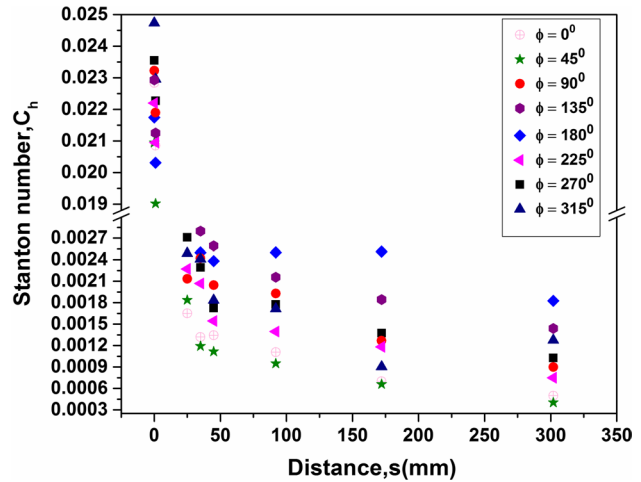


Fig. 13 The variation of Stanton number along the length of the model at $\alpha=5^\circ$ flying at Mach 7.25 for different angles of rotation in steps of 45°

distributions along the blunt cone model for different angles of rotation are shown in Fig. 12 at 5 degree angle of attack. The Stanton number was calculated from measured heat transfer value and free stream properties. The variation of Stanton number along the length of the model for $\alpha=5^\circ$ is shown in Fig. 13. The Stanton number follows the same trends as like heat transfer rate along the length of the model. The higher Stanton number was observed for $\phi = 180^\circ$ as compared to other angle of rotation. From the results, it shows that maximum heat transfer rate occurs at the stagnation point. This is due to large amount of kinetic energy gets dissipated as internal energy, hence causing the temperature

to rise when it crosses the strong shock wave in front of blunt model. The Stanton number decreased along the length of the model like heat transfer due to the increase in the velocity gradient and the increase in the growth of boundary layer thickness from the nose to corner.

4 Conclusions

The experiments were conducted at different angles of attack for different angles of rotation from $\phi=0^\circ$ to 360° in steps of 45° . All experiments were carried out in DRDL shock tunnel at flow Mach number of 7.25. Heat transfer measurement

with vacuum sputtered thin film gauge technique was accomplished in shock tunnel. The measured stagnation point heat transfer was lower for Mach number 7.25 when compared with the Fay-Riddell correlation. From the experimental results, it was found that heat transfer rate was essentially dependent on free stream Mach number and body shape. The measured heat flux from the repeat test had maximum standard deviation of 3.7%. At $\alpha = 5^\circ$, the heat transfer rate was higher when the angle of rotation $\phi = 180^\circ$ (windward) than the other cases ($\phi = 0^\circ, 45^\circ, 90^\circ, 135^\circ, 270^\circ, 315^\circ$). This higher heat transfer rate was due to higher density ratio across the detached shock wave and proximity of shock wave (i.e. shock layer thickness) closer to the blunt model.

References

- Charless G (1984) Miller experimental and predicted heating distributions for bionics at incidence in air at Mach 10, NASA 2334. Langley Research Center Hampton, Virginia
- Saito T, Menezes V, Kuribayashi T, Sun M, Jagadeesh G, Taka Yama K (2004) Unsteady convective surface heat flux measurements on cylinder for CFD code validation. *Shock Waves* 13:327–337. <https://doi.org/10.1007/s00193-003-0223-0>
- Chang PK (1970) Separation of flow. Pergamon Press, Oxford
- Ratan J, Jagadeesh G (2015) Investigations on supersonic combustion in a combustion-driven shock tunnel. *Proc IMechE G J Aerosp Eng*
- Liu J, Hou Z, Chen X, Zhang J (2013) Experimental and numerical study on the aero-heating characteristics of blunted waverider. *Appl Therm Eng* 51:301–314
- Shimshi JP, Gerald D (1995) Aerodynamic heating to spherically blunted cones at angle of attack. *J Spacecr Rockets* 32(3)
- Reddeppa P, Gai SL (2011) Measurement of heat transfer rate on backward-facing steps at hypersonic Mach number. *J Thermophys Heat Transf* 25(3)
- Kuribayashi T, Ohtani K, Takayama K, Menezes V, Sun M, Saito T (2007) Heat flux measurement over a cone in a shock tube flow. *Shock Waves* 16:275–285. <https://doi.org/10.1007/s00193-006-0068-4>
- Srinivasan K, Desikan SLN, Saravanan R, Kumar A, Maurya PK (2016) Fore-body and base heat flux measurements on a typical crew module in short duration impulse facilities. *Appl Therm Eng* 103:842–854
- Hollis BR, Perkins JN (1996) Hypervelocity heat-transfer measurements in an expansion tube. In: Proceedings of the 19th AIAA advanced measurement and ground testing technology conference June 18–20, 1996/New Orleans, LA.
- Kumar R (2014) Design, fabrication and Novel calibration techniques for heat transfer gauges during short duration transient measurement. PhD thesis, IIT Guwahati
- Hubner JP, Carroll BF, Schanze KS (2002) Heat-transfer measurements in hypersonic flow using luminescent coating techniques. *J Thermophys Heat Transf* 16(4)
- Kidd CT (1990) Recent developments in high heat-flux measurements at the AEDC. In: Proceedings of the 36th international instrumentation symposium, pp. 477–492.
- De Luca L, Guglieri G, Cardone G, Carlomagno GM (1995) Experimental analysis of surface flow on a delta wing by infrared thermography. *AIAA J* 33:1510
- Mosharov V, Orlov A, Radchenko V (2003) Temperature sensitive paint (TSP) for heat transfer measurement in short duration wind tunnels. In: Proceedings of the 20th international congress on instrumentation in aerospace simulation facilities (ICIASF 03), 25–29 August 2003, pp. 351–356.
- Nagai H, Oumi S, Asai K, Nakaita K (2006) Effect of temperature-sensitive paint layer on global heat transfer measurement in hypersonic flow. *J Visual Soc Jpn* 26(1):201–204
- Saiprakash M, Senthil Kumar C, Balu G, Shanmugam V, Rampratap SP, Kadam Sunil G (2019) Heat transfer rate and surface pressure measurements in shortduration hypersonic flow. *Aeronaut J* 123(1269):1857–1880. <https://doi.org/10.1017/aer.2019.116>
- Hollis BR (1995) User's manual for the one-dimensional hypersonic experimental aero thermodynamic (1DHEAT) data reduction code. NASA CR-4961
- Cook WJ, Felderman EJ (1966) Reduction of data from thin film heat transfer gauge a concise numerical technique. *AIAA J* 4:561–562
- Fay FR, Riddell JA (1958) Theory of stagnation point heat transfer in dissociated air. *J Aeronaut Sci* 25(2):73–85
- Saiprakash M, Senthil Kumar C, Balu G, Shanmugam V, Rampratap SP, Kadam Sunil G (2019) Convective heat-transfer rate and surface pressure distribution over a cone model at hypersonic speeds. *Proc Inst Mech Eng G J Aerosp Eng* 233(10):3649–3664

Publisher's Note Springer Nature remains neutral with regard to jurisdictional claims in published maps and institutional affiliations.